

Partial growth hormone insensitivity and dysregulatory immune disease associated with *de novo* germline activating *STAT3* mutations.

Mariana Gutiérrez¹, Paula Scaglia¹, Ana Keselman¹, Lucía Martucci¹, Liliana Karabatas¹, Sabina Domené¹, Miguel Blanco², Nora Sanguineti¹, Liliana Bezrodnik³, Daniela Di Giovanni³, María Soledad Caldirola³, María Esnaola Azcoiti³, María Isabel Gaillard³, Lee A. Denson⁴, Kejian Zhang⁵, Ammar Husami⁵, Nana-Hawa Yayah Jones⁶, Vivian Hwa⁶, Santiago Revale⁷, Martín Vázquez⁷, Héctor Jasper¹, Ashish Kumar⁸, Horacio Domené¹.

(1) Centro de Investigaciones Endocrinológicas ‘Dr César Bergadá’ (CEDIE) CONICET – FEI –División de Endocrinología, Hospital de Niños Ricardo Gutiérrez, Buenos Aires, Argentina. (2) Endocrinología, Hospital Universitario Austral, Buenos Aires, Argentina. (3) Inmunología, Hospital de Niños Ricardo Gutiérrez, Buenos Aires, Argentina. (4) Gastroenterology, Hepatology and Nutrition, Cincinnati Children’s Hospital Medical Center, Cincinnati, OH, USA. (5) Human Genetics, Cincinnati Children’s Hospital Medical Center, Cincinnati, OH, USA. (6) Division of Endocrinology, Cincinnati Center for Growth Disorders, Cincinnati Children’s Hospital Medical Center, Cincinnati, OH, USA. (7) Instituto de Agrobiotecnología de Rosario (INDEAR), CONICET, Rosario, Argentina. (8) Division of BM Transplantation and Immunodeficiency, Cincinnati Children’s Hospital Medical Center, Cincinnati, OH, USA.

Corresponding author:

Dr. Horacio Domené
 Centro de Investigaciones Endocrinológicas “Dr. César Bergadá” (CEDIE)
 CONICET – FEI – División de Endocrinología, Hospital de Niños Ricardo Gutiérrez
 Gallo 1330 – C1425EFD Buenos Aires
 Tel. (+54-11) 4963-5931 – Fax: (+54-11) 4963-5930
 E-mail: hdomene@cedie.org.ar

Abstract

Germinal heterozygous activating *STAT3* mutations represent a novel monogenic defect associated with multi-organ autoimmune disease and, in some cases, severe growth retardation. By using whole-exome sequencing, we identified two novel *STAT3* mutations, p.E616del and p.C426R, in two unrelated pediatric patients with insulin-like growth factor (IGF)-1 deficiency and immune dysregulation. The functional analyses showed that both variants were *gain-of-function*, although they were not constitutively phosphorylated. They presented differences in their dephosphorylation kinetics and transcriptional activity under interleukin-6 stimulation. Nonetheless, both variants increased their transcriptional activities in response to growth hormone (GH) treatment, in agreement with the partial response to GH therapy observed in the patients. This study highlights the broad clinical spectrum of patients presenting activating *STAT3* mutations and explores the underlying molecular pathway responsible for this condition, suggesting that different mutations may drive increased activity by slightly different mechanisms.

Abstract words count: 139.

Highlights

- WES performed in two unrelated patients reveals two novel *STAT3* variants.
- Both variants were associated to severe growth failure and immune dysregulation.
- Functional studies showed they are activating variants.
- They respond *in vitro* differentially to growth hormone and interleukin-6.
- They may drive increased transcriptional activity by slightly different mechanisms.

Keywords

STAT3, IGF1 deficiency, growth hormone insensitivity, activating mutations, immune dysregulation.

1. Introduction

Growth failure associated with severe primary insulin-like growth factor 1 (IGF1) deficiency is characterized by an insufficient production of IGF1, notwithstanding adequate secretion of growth hormone (GH). The classic form of severe primary IGF1 deficiency (IGFD) is Laron syndrome, where a homozygous or compound heterozygous mutation in the gene encoding the GH receptor (GHR) leads to low or undetectable IGF1 levels (1). Other well defined causes of IGFD are defects in genes encoding post-GHR signaling components, including the signal transducer and activator of transcription (STAT)-5b (2), the IGF1 (3) and the acid-labile subunit (ALS) (4). Recently, activating mutations in the *STAT3* gene were described in children with severe growth failure associated with a spectrum of early-onset autoimmune disease (5, 6, 7). STAT3 is a cytosolic protein involved in intracellular signaling transduction from cytokines, including several interleukins (IL), interferons (IFN α/β and γ) and growth factors (8). It contains several domains, a coil-coiled, a DNA binding, a SH2 and a transactivation domain and it is involved in many biological processes, such as cell growth, apoptosis, organogenesis, inflammation, infection and oncogenesis (9). Response to cytokines and growth factors is mediated by JAK activation, which in turn, phosphorylates specific tyrosine residues of the receptor. The phosphotyrosine residues constitute the docking site for the SH2 domain of the STAT3 protein, leading to JAK-mediated STAT3 phosphorylation and dimer formation. STAT3 dimers translocate to the nucleus, bind to DNA and induce gene transcription (10).

Heterozygous dominant-negative mutations of STAT3 are causal of autosomal dominant hyperimmunoglobulinemia E syndrome (AD-HIES) (8). Patients with AD-HIES present neonatal eczema, skin abscesses, mucocutaneous candidiasis, recurrent pneumonia, skeletal and connective tissue abnormalities, brain alterations, and distinctive coarse face (11). STAT3 mutations identified in AD-HIES patients affect mainly the SH2, DNA-binding or transactivation domains.

Germinal heterozygous *STAT3* gain-of-function (GOF) mutations have been recently described in patients with a broad spectrum of clinical manifestations, including type I diabetes, enteropathy, autoimmune cytopenia, hypothyroidism, arthritis, and interstitial lung disease (5, 6, 7). Most patients with STAT3 GOF mutations have short stature and

delayed puberty. Activating STAT3 germline mutations are located in the DNA-binding, SH2, transactivation or coiled-coil domains.

We report two novel heterozygous *de novo* STAT3 mutations in two unrelated patients with severe growth failure and IGF1 deficiency. We have evaluated the effects of these variants on the endocrinological and the immunological system and characterized the *in vitro* functional activity in response to GH and IL-6 stimuli.

2. Subjects and methods

2.1 Case reports

Patient 1

Patient 1 was a female, the second daughter from healthy non-consanguineous parents of normal height, born at term with normal weight (3.155 g, -0.18 SDS) and low birth length (44 cm, -2.76 SDS) (Table 1). Congenital autoimmune hypothyroidism was diagnosed with anti-thyroid antibodies persistently positive since birth. In the first two years of life she developed descamative eczema, chronic diarrhea, an episode of *Citrobacter spp* urinary tract infection, recurrent oral candidiasis, lymphocytic interstitial pneumonia with non-necrotizing granulomas associated with severe respiratory infections that required permanent oxygen supply and over 30 hospitalizations. She was referred to the pediatric endocrinologist at 2.4 years of age, when she presented a height of -6.4 SD. The immunological evaluation showed IgG levels between -1 to -2 SDS for age, with elevated IgA (>2 SDS), normal IgM and non-detectable IgE levels (Table 1). Lymphocyte subsets, including CD3⁺, CD4⁺, CD8⁺, CD19⁺, CD3⁻, CD56⁺ and regulatory T cells (CD4⁺ CD25⁺⁺CD127^{low}Foxp3⁺ Tregs), were normal. Her cytokine profile revealed absence of Th17 with CD4⁺ T cells skewed to Th2. The patient also had elevated prolactin and GH serum levels, associated to non-detectable IGF1 and normal IGFBP3 levels. She underwent an IGF generation test with recombinant human (rh) GH (33 µg/kg.day) for 7 days which showed a limited increase in IGF1 and normalization of IGFBP3 levels (Table 1). She received levothyroxine treatment since 20 days of age and started rhGH treatment (0.43 mg/kg.wk) at 2.5 years, gaining 1.4 SDS in 2 years of treatment and increasing IGF1 levels to 240 ng/ml (Supplementary Figure 1). She also received oral meprednisone, prophylactic trimethoprim-sulfamethoxazole and intravenous γ globulin treatments. At the age of 3.2

years oral sirolimus was added but was replaced by oral cyclosporine because of lymphedema complications. The patient died at 4 years of age, 18 days after a bone marrow transplantation with a matched unrelated donor due to a multiple organ failure.

Patient 2

Patient 2 was a male, the second child from non-consanguineous parents, born at term with normal weight and birth length (Table 1). His parents and older brother are of normal stature and healthy. At 2 weeks of life patient was hospitalized for RSV bronchiolitis with hypoxia. In the first two years of life, he developed failure to thrive associated with chronic, intractable diarrhea, intermittent vomiting, abdominal distention, and severe eczema. Endoscopy at 2 years of age indicated marked lymphocytic gastritis and basal cell hyperplasia of the esophagus and stomach consistent with gastritis; mild lymphoid nodularity was observed in the duodenum. Acquired hypothyroidism was diagnosed at age 2, and levothyroxine (L-T4) therapy started. At the age of 3, his height was -5.4 SD. Prior treatments included topical tacrolimus, sulfasalazine, inhaled corticosteroids, bronchodilators and proton pump inhibitors. He was also treated with a variety of immune-suppressive agents including prednisolone, Sirolimus, and Abatacept, all with minimal response. Growth improved but remained poor. The immunological phenotype was similar to that of Patient 1 (Table 1) with normal IgG and IgM levels, high IgA and non-detectable IgE levels. Lymphocyte subsets, including FOXP3+, Tregs and TH17 were all normal. Endocrine evaluation was notable for relatively high GH serum levels, normal prolactin, undetectable IGF1 and low IGFBP3 levels. The patient's hypothyroidism was not well-controlled. TSH values rarely normalized despite L-T4 supplementation of ~5 mcg/kg/day. At age 6, the patient passed a pseudo-malabsorption test suggesting non-adherence to prescribed L-T4 therapy rather than malabsorption of thyroxine compound. At age 7, he was started on rhGH (0.3 mg/kg/day) showing a partial response with gain of height SDS from -2.90 to -2.48 within 1.4 years of treatment. IGF1 has normalized to near 10-25th centile for age. Previous gain in height SDS from -5.4 was attributed to thyroxine and immunologic treatments.

153 **Table 1:** Clinical characteristics of patients with *de novo* STAT3 mutations.

		Patient 1 (female)	Patient 2 (male)
Birth	Gestational Age (weeks)	38	38
	Birth weight (g)	3155	3586
	Birth length (cm/SDS)	44 (-2.76)	50.8 (-0.75)
First visit	Chronological Age (years)	2.5	3.0
	Height (SDS)	-6.4	-5.4
	Weight (SDS)	-3.4	-2.7
Clinical features		Congenital autoimmune hypothyroidism, descamative eczema, chronic diarrhea, recurrent oral candidiasis, severe respiratory infections	History of IPEX-like syndrome with dermatitis, chronic diarrhea, colitis, autoimmune hypothyroidism
Immunological evaluation	IgG (RR: 760-1348 mg/dL)	637	760
	IgA (RR: 40-132 mg/dL)	389	211
	IgM (RR: 79-131 mg/dL) (mg/dL)	103	134
	IgE (RR: 8-32 UI/mL)	<5	<1
	CD3/CD4/CD8/CD19/CD3CD56 (%)	49/34/14/42/8	82/35/45/12/nd
	FOXP3/Treg CD127/Th17	N/N/low	N/N/N
Endocrine evaluation	GH (ng/ml)	20	----
	IGF1 (ng/ml) basal (RR: 35-160)	<12	<25
	post IGF-GT (rhGH for 7d)	20	

	IGFBP3 (µg/ml) basal (RR: 1.7-4.2)	1.0	0.5
	post IGF-GT (rhGH for 7 d)	2.2	
	Prolactin (ng/ml) (RR: 2-15)	30,6	----
	TSH (mIU/ml) (RR: 0.5-6.5)	238	364
	FT4 (ng/dl) (RR: 0.8-2.0)	0.4	0.2
	TPO-Ab / TG-Ab (IU/ml) (RR:<20/<20)	83 / 48	>1000 / 165
	Dose	0.43 mg/kg.wk	0.3 mg/kg.d
rhGH treatment	Height gain (SDS) / Period (years)	1.4 / 2	0.42 / 1.4
	IGF1 (ng/ml)	240	
	IGFBP3 (µg/ml)	4.4	
		c.1847_1849delAAG	c.1276T>C
Molecular studies	WES: Heterozygous <i>de novo</i> <i>STAT3</i> variants	(p.Glu616 del)	(p.Cys426Arg)
		SH2 domain	DNA binding domain

154 RR: Reference range. N: Normal. nd: Not determined

155 For Patient 1, height SDS was based on Argentinean growth references (36) and for Patient
156 2, on 2000 CDC growth charts (37).

157

158 2.2 Molecular studies

159 Genomic DNA from patients and relatives were extracted from venous peripheral blood
160 (12). Using a candidate gene approach, *STAT5B* and *FOXP3* genes were analyzed for P1
161 and P2 respectively, by PCR amplification followed by Sanger sequencing. Whole Exome
162 Sequencing for patient 1 was performed using Illumina HiSeq1500 at the Instituto de
163 Agrobiotecnología de Rosario (INDEAR)-CONICET (Rosario, Argentina) in a quartet-
164 design, including the index case, her parents, and her healthy sister, using Illumina Nextera
165 Exome V1.2 kit (45 Mb - 214,405 exons) for exome capture. WES for Patient 2 and
166 unaffected parents was performed through the DNA Sequencing and Genotyping Core at
167 Cincinnati Children's Hospital Medical Center (Cincinnati, Ohio, USA), employing

Illumina HiSeq2500. Stringent filtering strategies for analyzing WES data include population frequency, pattern of inheritance, and specific filters for immune candidate genes. STAT3 likely pathogenic variants were identified in the index cases, and confirmed by Sanger sequencing in patients and family members (primers used are available upon request).

2.3 *In silico* bioinformatics analysis

STAT3 variants were analyzed *in silico* to predict their effects on protein function. For this purpose, different bioinformatics tools were used: PolyPhen-2 (13), SIFT (14), Mutation Taster (15), MutPred (16), and SNAP² (17). The following NCBI reference sequences were used: NG_007370.1 (gene), NM_139276.2 (mRNA) and NP_40763.1 (protein). Different databases were used to evaluate the presence of the *STAT3* variants found in the patients: dbSNP (the NCBI database for Short Genetic Variation, http://www.ncbi.nlm.nih.gov/SNP/snp_ref.cgi?locusId=3483), COSMIC (the Catalogue Of Somatic Mutations In Cancer, <http://cancer.sanger.ac.uk/cosmic>) and ExAC (the Exome Aggregation Consortium, <http://exac.broadinstitute.org>). A multiple sequence alignment was done with PRALINE program (<http://www.ibi.vu.nl/programs/pralinewww/>) using NCBI reference sequences. *In silico* structural models for STAT3 variants were based on the crystal structure of the mouse STAT3B homodimer bound to DNA (PDB ID: 1BG1) (18). Protein structure was visualized using the molecular graphics program PyMOL (PyMOL Molecular Graphics System, Version 1.8.4.0, Schrödinger, LLC, <http://www.pymol.org/>) which was also used to generate *in silico* the studied mutations. Side chain conformation for p.C426R was selected from the PyMOL backbone-dependent rotamer library that resulted in less steric clashes with surrounding residues.

2.4 Site-directed mutagenesis

Gene variants were introduced into a commercial plasmid (pCMV6-Entry, RC215836, Origene, Rockville, MD, USA) containing the wild-type (WT) *STAT3* cDNA (NM_139276), using the Quick Change II XL Site-Directed Mutagenesis Kit (Agilent Technologies, Santa Clara, CA, USA) and primers listed in Supplementary Table 1. All constructs were verified by sequencing.

2.5 Cell Culture and transfections experiments

HEK293-T cells were routinely grown in Dulbecco's modified Eagle's medium (DMEM) supplemented with 10% fetal calf serum, penicillin (100 units/mL), streptomycin (100 µg/mL) and L-glutamine (2 mM) at 37°C in a humidified atmosphere with 5% CO₂. For transfection experiments, HEK293-T cells were seeded at a density of 2×10^5 cells/well in a 24-multi well plate, grown to approximately 70-90% confluence, and transiently transfected with 500 ng Empty-pCMV6, or with a combination of 250 ng pcDNAI_Amp-GHRfl (19) and 250 ng vector carrying WT-STAT3 or variants using Lipofectamine 3000 reagent (Invitrogen, Carlsbad, CA, USA). After 24 h transfection, cells were washed and serum starved for 6 h before a 15, 30 or 120-min treatment with 200 ng/ml recombinant human (rh) GH (Sandoz, Olivos, Argentina) or 20 ng/mL IL-6 (Gibco, Grand Island, NY, USA). Transfection experiments were performed in duplicates, at least four independent times.

2.6 Luciferase reporter assay

HEK293-T cells were seeded as described above and cotransfected with 125 ng of Cignal reporter assay constructs (Cignal STAT3 Reporter Assay kit (LUC), Qiagen, CA, USA), 187.5 ng of WT or mutant STAT3 containing plasmids and 187.5 ng of pcDNAI_Amp-GHRfl using the Lipofectamine 3000 transfection reagent. After 24 h transfection, cells were washed and serum starved for 6 h before 18-h treatment with 200 ng/mL rhGH or 20 ng/mL IL-6. STAT3 reporter activity was assessed using a dual luciferase reporter assay system (Promega, Madison, WI, USA) according to the manufacturer's instructions. The *renilla* plasmid was used to normalize transfection efficiency. Results represent the ratio of reporter (firefly) to control (*renilla*) luciferase or are normalized as fold-change in the ratio as compared with WT-STAT3 plasmid. Data are presented as the mean \pm SEM of at least five independent experiments.

2.7 Western Immunoblot (WIB)

The effects of GH and IL-6 on STAT3 phosphorylation status in HEK293-T cells expressing GHR were examined by WIB analysis. Cells were starved for 6 hours in serum-

free medium and then stimulated with 200 ng/mL rhGH or 20 ng/mL IL-6 at 37°C for 15, 30 and 120 minutes. After treatment, cells were washed with PBS and lysed in RIPA lysis buffer (1× phosphate-buffered saline, 1% v/v Nonidet P-40, 0.1% w/v SDS, 10 mg/ml phenylmethylsulfonyl fluoride, 1 mM sodium orthovanadate and protease inhibitor mixture). In a separate experiment designed to study dephosphorylation kinetics, after 30 minute-treatment with 200 ng/mL rhGH or 20 ng/mL IL-6 at 37°C the stimuli were removed and the cells were washed with PBS and incubated for 15, 30 or 120 minutes at 37°C in serum-free medium before solubilization. Extracts containing equal amounts of proteins, determined by the Bradford method (Bio-Rad, Michigan, USA), were separated by SDS-PAGE (12% acrylamide) and transferred to polyvinylidenedifluoride membranes (EMD Millipore, Billerica, MA, USA). Phosphorylation was detected using an anti-phospho-STAT3 (Tyr705) rabbit monoclonal antibody (Cell Signaling Technology, Danvers, MA, USA) and protein abundance of STAT3, using a rabbit monoclonal antibody against STAT3 (Cell Signaling Technology, Danvers, MA, USA). The signal was developed with donkey anti-rabbit Ig-horseradish peroxidase (GE Healthcare Life Sciences, Freiburg, Germany) by chemiluminescence using 20X LumiGLO Reagent (Cell Signaling Technology, Danvers, MA, USA).

2.8 Statistical Analysis

All experiments were repeated at least four times. For the luciferase assays, mean \pm SEM of results from multiple experiments of the same study are reported. Data were analyzed by Student's paired t test where appropriate, and significance was set at $P < 0.05$.

3. Results

3.1 Whole Exome Sequencing: Two novel variants identified in the *STAT3* gene

In patients 1 and 2, the short stature, immunological and endocrinological evaluations, suggested possible defects in the *STAT5B* (2, 20) and *FOXP3* (21, 22), respectively, but candidate gene analyses were unrevealing. WES analysis was, therefore, undertaken.

In patient 1, WES performed in a quartet-design (patient, parents and healthy sister) revealed 42639 variants in 13110 genes. We applied different filtering strategies including mutation consequence (nonsense, missense, deletion or insertion in coding sequence),

population frequency (<1%), inheritance pattern (autosomal recessive or *de novo*) and a 250-candidate gene list considering the pathway involved. After a critical review of the literature and a final step of manual curation of the variants, we selected a heterozygous in frame 3 bp deletion in *STAT3* gene as the most likely candidate variant causing the observed phenotype of the patient. The variant c.1847_1849delAAG is predicted to result in deletion of glutamic acid 616 (p.Glu616del), located in the SH2 domain of the protein. WES analysis of Patient 2 and unaffected parents led to the identification of a private, *de novo*, heterozygous *STAT3* variant, c.1276T>C, exon 14, as the top candidate variant in the patient. The c.1276T>C generates a predicted missense substitution, p.Cys426Arg, in the DNA binding domain of the protein. Analysis of parental DNA samples showed that both mutations had arisen *de novo*. According to bioinformatic algorithms and the ACMG recommendations (23), both variants were classified as likely pathogenic (Supplementary Table 2). The variant p.E616del has only been reported as a somatic mutation causing large granular lymphocytic (LGL) leukemia (COSMIC database) whereas variant p.C426R is absent from public databases of genetic variation (dbSNP, ExAC and COSMIC). The analysis of positional conservation of STAT3 residues by multiple sequence alignment from six species (human, chimpanzee, rhesus, mouse, chicken and zebrafish) showed that both residues C426 and E616 are highly conserved within the DNA binding and the SH2 domains, respectively, among species (Figure 1). The E616 is also conserved among STAT1 and STAT2, in contrast to C426 which is not conserved among STATs proteins. Figure 2A shows an illustration of the three-dimensional structure of the mouse Stat3b homodimer bound to DNA. The residues corresponding to the reported variants are shown in magenta. C426 is located in a region without known structure, within a stretch of 19 amino acids that is flanked by β -sheets. Although E616 is located within the SH2 domain, it is close to the DNA binding surface and interactions between the STAT3 protein and the DNA duplex may involve this residue (Figure 2A).

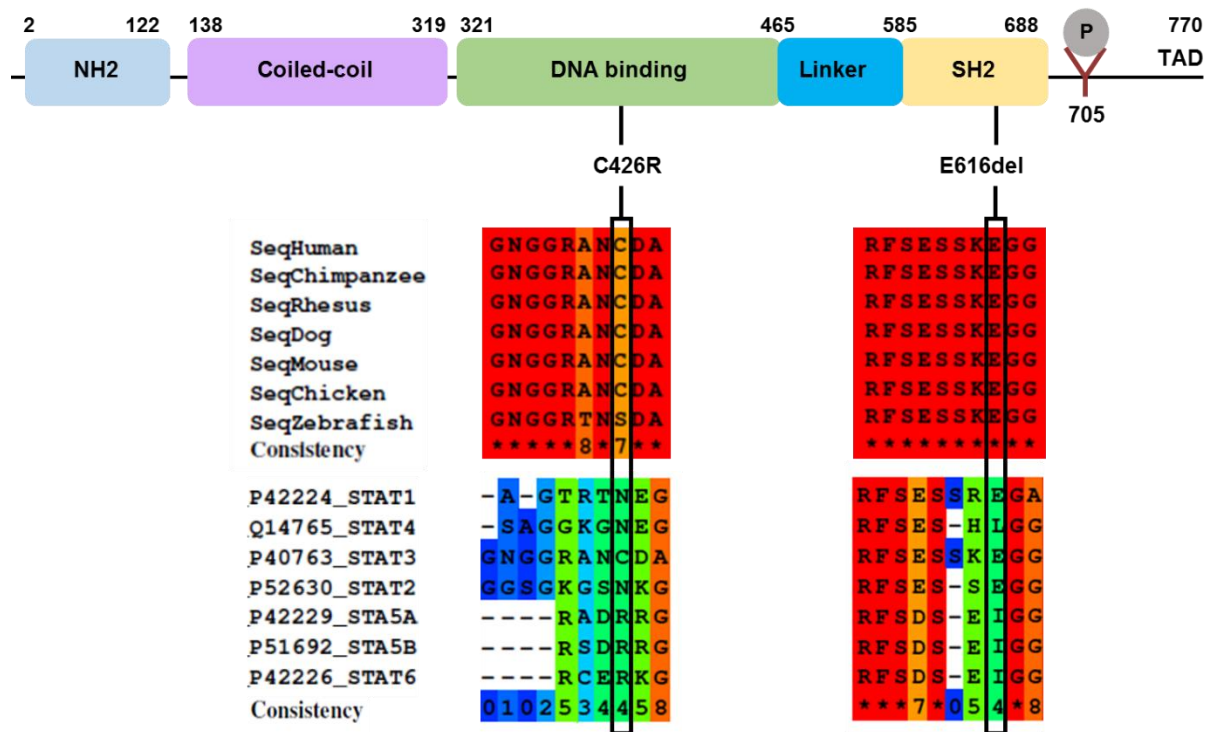


Figure 1: Schematics of human STAT3. The position of the two *de novo* mutations are shown below the STAT3 domains. Multiple sequence alignments among different species and among STAT proteins were done with PRALINE software. The color scheme indicates the least conserved alignment position (dark blue), to the most conserved alignment position (red).

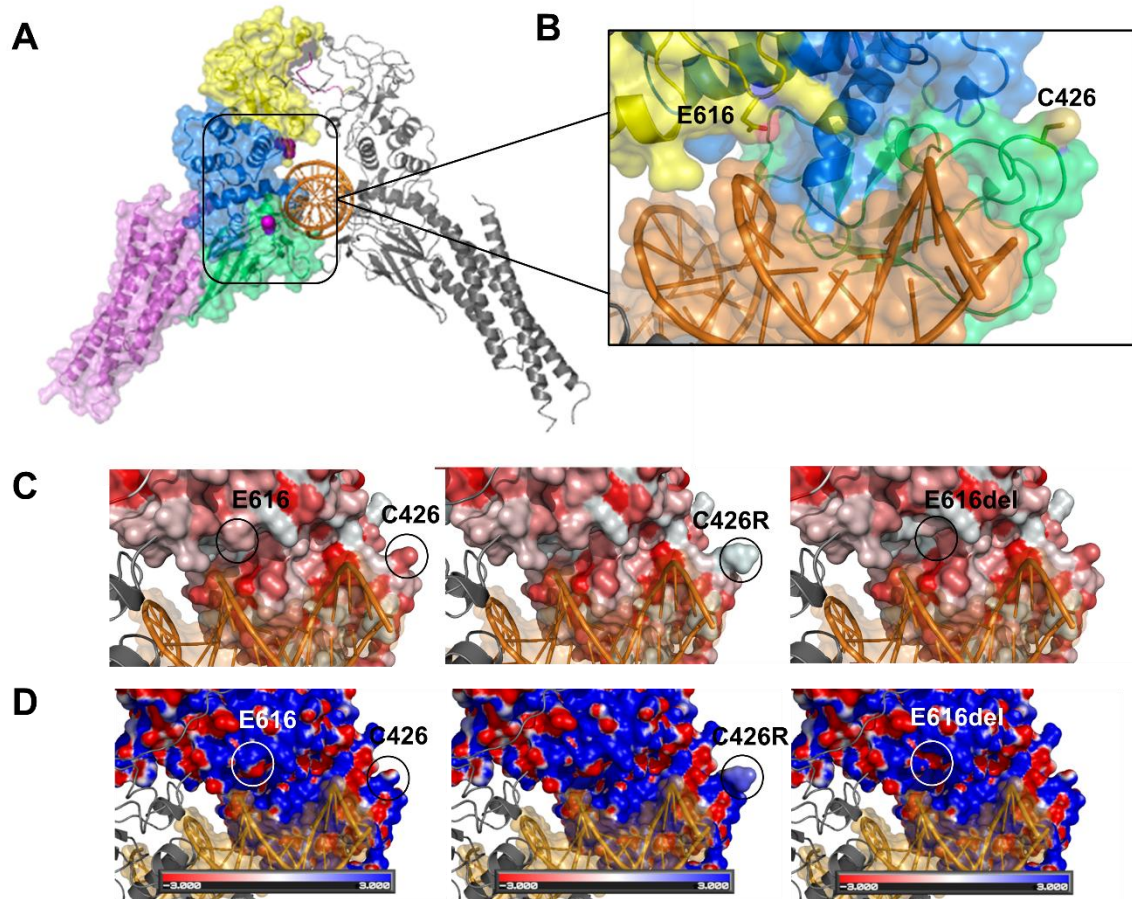


Figure 2: **A)** Structural model of the STAT3 dimer bound to DNA (PDB ID: 1BG1) (18) in cartoon representation. Individual domains are color coded as in Figure 1 only on the left chain. Variant residues under study are shown as space-filling mode in magenta. **B)** The structure has been rotated and expanded to show residues E616 and C426 (sticks) close to the DNA duplex surface. **C)** Surface representation of the predicted hydrophobicity of WT-STAT3 (left) and variants p.C426R (center) and p.E616del (right). Coloring was achieved using the color_h.py python script in Pymol, and the color scale is based on the Eisenberg normalized hydrophobicity scale (34) where hydrophilic residues are lighter/white, and hydrophobic residues are darker/red. Both variants show an increase in the hydrophobicity surface in regions where the residues were substituted or deleted. **D)** Electrostatic potentials are mapped onto the molecular surfaces of WT-STAT3 and mutants, with negative potentials colored red and positive potentials colored blue. The electrostatic potentials were

calculated and visualized using APBS plugin -Adaptive Poisson–Boltzmann Solver (35)- in Pymol. The variants (center and right) show an increase in the positive electrostatic potential on the DNA binding surface compared to WT-STAT3 (left).

3.2 STAT3 p.E616del and p.C426R are constitutively activated variants that further increase their transcriptional activities in response to GH.

To investigate possible functional consequences of p.E616del- and p.C426R-STAT3 variants, we evaluated the activity of each mutant using a STAT3-responsive dual-luciferase reporter assay. Constructs encoding the identified *STAT3* mutations, a *loss-of-function* -LOF- mutation described in hyper IgE syndrome, p.R423Q (24), and WT-STAT3 were generated and transiently transfected into cultured HEK293-T cells expressing GHR. Expression of p.E616del and p.C426R mutants resulted in a significant increase in reporter activity ($P < 0.05$) in comparison to WT-STAT3 or LOF-STAT3 under non-stimulated conditions (Figure 3A), suggesting that these mutants are constitutively activated. The effect of GH on the transcriptional activity of p.E616del and p.C426R was also evaluated. In WT-STAT3 transfected cells, GH stimulation resulted in an 8-fold increase above basal levels. For constitutively activated p.E616del and p.C426R, GH treatment increased luciferase activities by 2- to 4-fold above the levels observed for WT-STAT3 (Figure 3B). Although HEK293-T constitutively express GHR, in our system GH was not able to stimulate luciferase production in cells not overexpressing GHR (data not shown). These results suggest that GH stimulation is specifically mediated by the GH receptor. IL-6 stimulation of WT-STAT3 induced the luciferase reporter gene 15- to 20-fold (Figure 3C). Both p.C426R and p.E616del variants showed ~2- to 2.5-fold increase in reporter activity under IL-6 stimulation (Figure 3B). However, the fold change relative to WT-STAT3 was significantly higher only for p.C426R variant (Figure 3C).

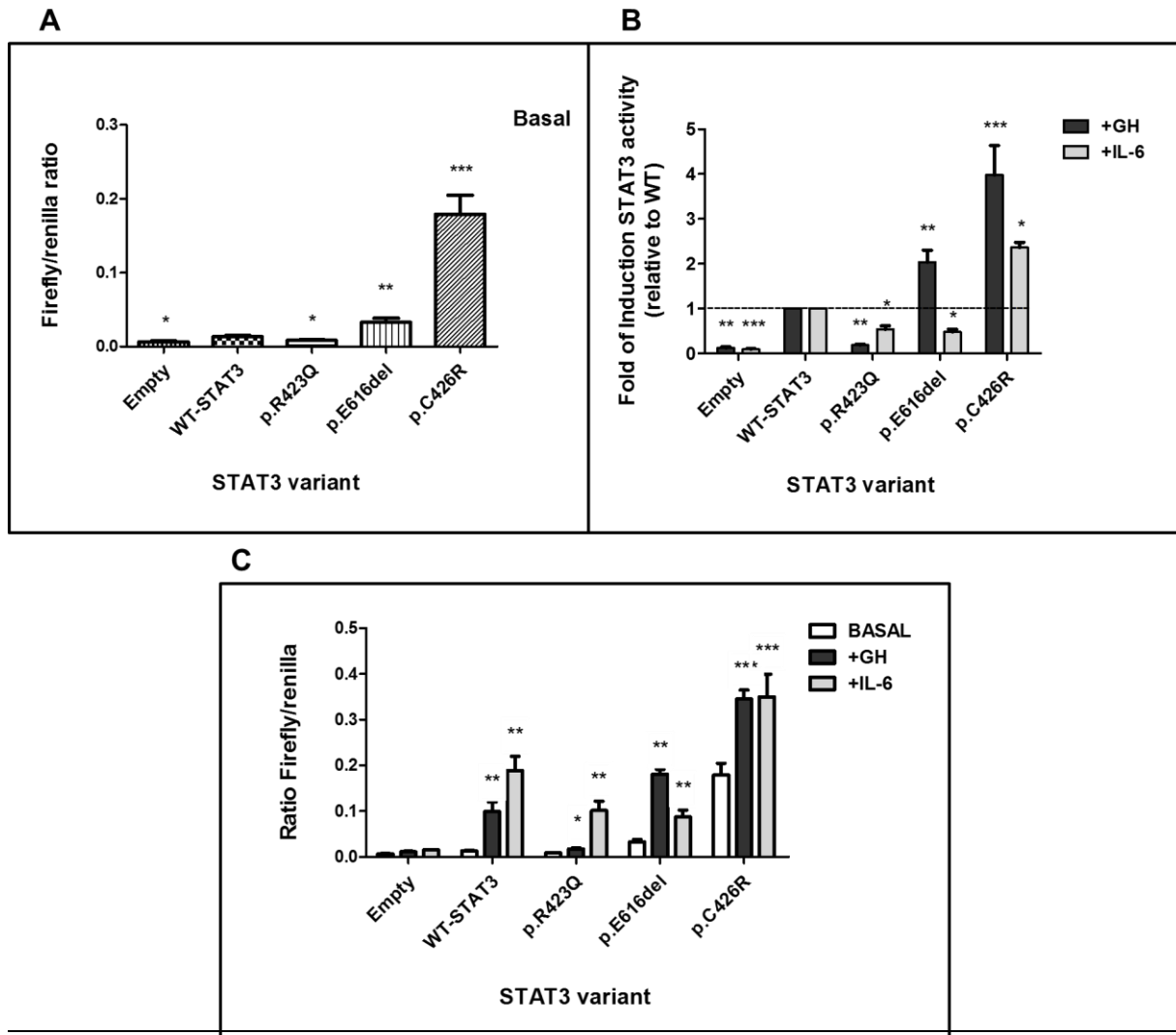


Figure 3. STAT3 transcription activity determined by luciferase reporter assay. **A)** STAT3 activity of WT and variants, p.E616del, p.C426R and LOF variant, p.R423Q, under non-stimulated conditions. Data represents the mean ratio of firefly/control luciferase activity for each construct \pm SEM (n=5). **B)** STAT3 activity of WT and mutants following 18h activation with GH (200 ng/mL, black) or IL-6 (20 ng/mL, gray). Data are presented as average fold of change relative to WT \pm SEM of at least 5 independent experiments. The dotted line represents a fold-change of 1 (no change from WT). **C)** The same experiment as B) but data are presented as the mean ratio of firefly/control for each construct \pm SEM (n=5) under GH (200 ng/mL, black) or IL-6 (20 ng/mL, gray) 18-h treatment in comparison with unstimulated conditions. * $P < 0.05$, ** $P < 0.01$, *** $P < 0.001$, t test.

3.3 The STAT3 variants are not constitutively phosphorylated and demonstrate different dephosphorylation patterns under GH and IL-6 treatments.

To further investigate the differences in the activation of p.E616del and p.C426R, we evaluated the effects of IL-6 and GH on Y705-STAT3 phosphorylation by WIB. Under basal conditions (unstimulated), STAT3 was not phosphorylated in either mutant (Figure 4). WT-STAT3 and both variants were phosphorylated in response to IL-6 and GH and dephosphorylation was not observed within the first 30 min of stimulation (Figures 4A and 4B). Phosphorylated 705Tyr- was still detectable up to 120 min of treatment. However, at this time-point, phosphorylation was diminished for WT-STAT3 (Figures 4A and 4B). A similar temporal pattern was observed for p.R423Q. This inactivating substitution is located in the DNA binding domain and the STAT3 loss of function is not a consequence of altered phosphorylation, as was previously reported (25).

Both STAT3 activating mutants exhibited different dephosphorylation kinetics under GH and IL-6 treatments. While p.C426R exhibited delayed dephosphorylation only under GH treatment (Figure 4A), p.E616del showed delayed dephosphorylation only when stimulated with IL-6 (Figure 4B). To study differences in STAT3 dephosphorylation kinetics, we removed GH or IL-6 stimuli after 30 min of treatment and cell lysates were then collected 15, 30 and 120 min after depletion. Cell lysates were analyzed by WIB (Figures 4C and 4D). No differences regarding the temporal dephosphorylation pattern were observed for WT-STAT3 and p.R423Q when GH or IL-6 were depleted from the media. In contrast to the previous observed results, when GH and IL-6 stimuli were maintained, no delayed dephosphorylation was observed for p.C426R and p.E616del once the stimuli were depleted from the media (Figures 4C and D).

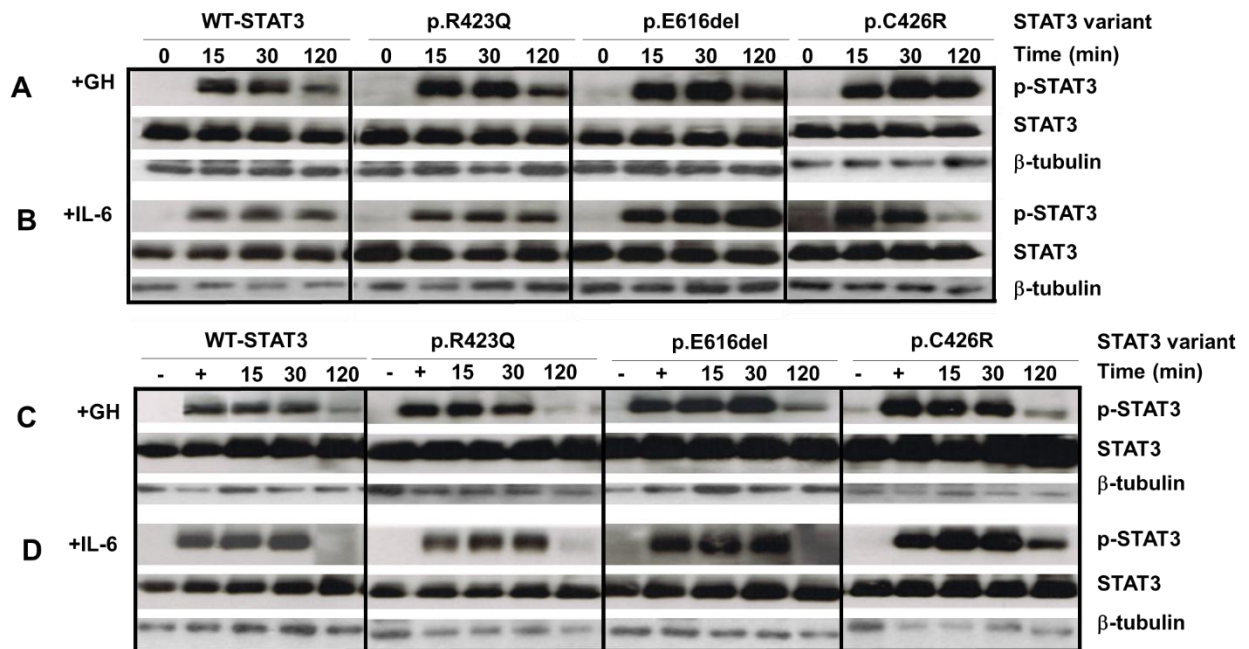


Figure 4. Western Blot of STAT3 expression and phosphorylation. WT-STAT3 and mutants were transfected in HEK293-T cells expressing GHR and p-STAT3 and total STAT3 were determined under basal (0 min) or stimulated conditions (15, 30, 120 min). GH (200 ng/mL) (A) and IL-6 (20 ng/mL) (B) induce phosphorylation of WT-STAT3 and mutants. p-STAT3 and total STAT3 were evaluated additionally at 15, 30 and 120 min after removing a 30-min treatment with GH (+, 200 ng/mL) (C) and IL-6 (+, 20 ng/mL) (D). β-tubulin was used as loading control. p-STAT3, phosphorylated STAT3.

4. Discussion

In this study, we presented two novel cases of IGF1 deficiency, severe short stature and immune dysregulation due to activating germline STAT3 mutations identified by WES. The two patients shared clinical features such as autoimmune hypothyroidism, dermatitis, chronic diarrhea and recurrent infections. They present a clinical phenotype overlapping with previously described patients with *STAT3* GOF mutations (5, 6, 7), as well as some clinical similarities to other single-gene immune dysregulation disorders, including autoimmune lymphoproliferative syndrome (ALPS), immunodeficiency polyendocrinopathy enteropathy x-linked (IPEX), IPEX-like disorders, and *STAT5B*-deficiency. Of note, patients with *STAT5B* LOF mutations present severe postnatal growth

failure and marked IGF1 deficiency as consequences of complete GH insensitivity, including poor responsiveness to GH treatment (2). In contrast, patient 1 had a good response to GH therapy. Good response to GH treatment was also reported in 2 other patients with activating *STAT3* mutations (5). To our knowledge, 15 out of 22 reported patients with available growth data (5, 6, 7, 26, 27, 28) (~68%, including our patients) had growth impairment (Supplementary Table 3 and Supplementary Figure 2) suggesting a disruptive role of *STAT3* GOF variants in GH signaling pathway. In consequence, we propose considering *STAT3* activating mutations as an additional monogenic cause of primary IGF-1 deficiency. Nonetheless, it is not possible to rule out the potential deleterious effects of the immune dysregulation (diabetes, hypothyroidism, recurrent infections) and the pharmacological treatments on the growth rate in these patients.

P1 died after hematopoietic stem cell transplantation (SCT). Unfortunately, SCT was also unsuccessful in two out of three other patients, who succumbed shortly after the procedure (5, 7, 26). This suggests that other therapeutic approaches, such as specific small-molecule *STAT3* inhibitors, are perhaps more appropriate therapies for these patients.

To evaluate the impact of these mutations on *STAT3* structure and activity we performed *in silico* and *in vitro* studies. Sequence alignments showed that C426 residue is located in a region containing basic amino acids in all *STAT* family proteins. *STAT5a*, *5b* and *6* have an arginine residue in the equivalent position to *STAT3* C426 (Figure 1), suggesting that the change C426R in the *STAT3* could be structurally tolerated. *In silico* mutagenesis of C426 by arginine using Pymol backbone-dependent rotamer library is predicted to cause an increase in the hydrophobicity in this region, compared to WT-*STAT3* (Figure 2B). Moreover, the calculation of electrostatic potential reveals an increase in the positively charged surface on the DNA-binding interface on p.C426R (Figure 2C), as expected for the substitution of cysteine for the positively charged arginine residue. Likewise, *in silico* deletion of E616 predicts an increase in the positive electrostatic potential at the proximity of the DNA-binding surface (Figure 2C). Therefore, both mutations would enhance the electrostatic interaction with the negatively charged DNA phosphate backbone, suggesting an increase in DNA binding affinity and, consequently, in an increased *STAT3* transcriptional activity.

425

426 *In vitro* characterization of both variants indicated they were GOF variants since they
427 activate STAT3 signaling pathway in absence of stimuli. As far as we know, the variant
428 p.E616del is the only activating deletion in STAT3 described in patients with this
429 syndrome. Although E616 is located within the SH2 domain, using molecular dynamics
430 simulations Husby *et al.* have predicted E616 as a key residue of monomer-B involved in
431 STAT3 protein-DNA interaction (29), consistent with our molecular modelling. Therefore,
432 enhanced activity of both variants, p.C426R and p.E616del, might be a consequence of
433 electrostatic effects caused by the gain of positive charges at the DNA-binding surface,
434 leading to increased DNA binding affinity and prolonged nuclear retention.

435 Each mutant responded differently to GH and IL-6 *in vitro*. When treated with IL-6, the
436 transcriptional activity of p.E616del increased compared to unstimulated conditions.
437 Nonetheless, this increase was lower than levels reached for WT-STAT3. This result is
438 consistent with previously reported STAT3 mutations located within the same region,
439 p.N646K (6) and p.T663I (5), where the significant increase in reporter activity under basal
440 conditions was not above the levels reached by WT-STAT3 after stimulation with IL-6. In
441 contrast, p.C426R had markedly elevated basal activity which was further increased with
442 GH and IL-6 stimulation, as reported for other mutations in the DNA binding domain, as
443 well as in the other protein domains (5, 6, 7). Therefore, increased basal STAT3 activity
444 does not imply that response to a stimulus is also increased. The response will most likely
445 depend on the type and location of the mutation and on the stimulus applied. In accordance
446 with these findings, dephosphorylation patterns were different for each variant depending
447 on the treatment. The p.C426R variant showed delayed dephosphorylation only under GH
448 stimulus, while for p.E616del, delayed dephosphorylation was observed only when
449 stimulated with IL-6. Delayed dephosphorylations were not observed in absence of stimuli,
450 hence both variants are accessible to nuclear phosphatases that recycle STAT proteins back
451 to the cytoplasm.

452 The mechanism underlying these dephosphorylation patterns most probably involve the
453 increased DNA affinity, which induces a faster DNA binding (on-rate) and sensitizes
454 STAT3 to cytokine stimulation, followed by a slow off-rate, which protects it from

inactivation by phosphatases, as has been suggested for the constitutively activated oncogenic Stat3 mutant (Stat3-C) (30).

STAT3 is ubiquitously expressed in different cell types, mediating the response of multiple cell receptors. It is possible that the critical intracellular concentration of activated STAT3 needed to elicit the cellular response varies depending on the nature of each STAT3 mutation. *In vivo*, cells are exposed to low level basal signaling that normally fails to trigger downstream events due to threshold sensitivities. With STAT3 activating variants, the increased transcriptional activity could be a consequence of a faster on-rate for DNA-binding, which could lower the threshold for pre-initiation complex formation. These differences in threshold and sensitivity levels of STAT3 variants to cytokines and growth factors, could also contribute to the broad spectrum of clinical manifestations among patients.

How these mutants affect STAT5b in the GH-signaling pathway requires further investigation. In most cell types, STAT5b and STAT3 play divergent and opposing effects on gene expression (31, 32). A previous study showed decreased STAT5 phosphorylation in patient-derived EBV-transformed cell lines carrying a STAT3 activating mutation (5). Authors suggest that STAT5 is negatively regulated by SOCS3, one of the main targets of STAT3. Nonetheless, other mechanisms can include the formation of nonfunctional STAT5b/STAT3 heterodimers, competition for common receptor docking sites and regulation for posttranslational epigenetic modifications, as was recently described for GOF-STAT1 mutations and their effects on STAT3 function (33).

Heterozygous *STAT3* GOF mutations result in a broad spectrum of clinical phenotypes, involving infectious and autoimmune diseases, growth failure and IGF1 deficiency. No clear genotype/phenotype correlation has been observed. In some inherited reported cases, family members carrying the same STAT3 GOF mutation presented a milder phenotype, or were even asymptomatic, suggestive of incomplete penetrance (5). As the effect of *STAT3* GOF mutations on the clinical phenotype is difficult to accurately predict, our present report emphasizes the importance of complementing genetic analysis with functional

studies to evaluate responsiveness to different stimuli, for a better understanding of potential therapeutic approaches.

5. Declaration of interest

The authors declare no conflict of interest.

6. Funding

This work was supported by PICT 2010 N° 1916 (ANPCYT), SANDOZ International GmbH Business Unit Biopharmaceuticals and the Fundación Alberto J. Roemmers.

7. Acknowledgements

We are grateful to the children, parents and relatives who agreed to take part in this study.

8. References

1. Laron Z. Lessons from 50 years of study of Laron syndrome. *Endocrine practice : official journal of the American College of Endocrinology and the American Association of Clinical Endocrinologists* 2015 **21** 1395–1402. (doi:10.4158/EP15939.RA)
2. Kofoed EM, Hwa V, Little B, Woods KA, Buckway CK, Tsubaki J, Pratt KL, Bezrodnik L, Jasper H, Tepper A, Heinrich JJ, & Rosenfeld RG. Growth Hormone Insensitivity Associated with a STAT5b Mutation. *New England Journal of Medicine* 2003 **349** 1139–1147. (doi:10.1056/NEJMoa022926)
3. Woods KA, Camacho-Hubner C, Savage MO, & Clark AJ. Intrauterine growth retardation and postnatal growth failure associated with deletion of the insulin-like growth factor I gene. *The New England journal of medicine* 1996 **335** 1363–1367. (doi:10.1056/NEJM199610313351805)
4. Domené HM, Bengolea S V, Martínez AS, Ropelato MG, Pennisi P, Scaglia P, Heinrich JJ, & Jasper HG. Deficiency of the circulating insulin-like growth factor system associated with inactivation of the acid-labile subunit gene. *The New England Journal of Medicine* 2004 **350** 570–577. (doi:10.1056/NEJMoa013100)
5. Milner JD, Vogel TP, Forbes L, Ma CA, Stray-Pedersen A, Niemela JE, Lyons JJ,

- Engelhardt KR, Zhang Y, Topcagic N, Roberson EDO, Matthews H, Verbsky JW, Dasu T, Vargas-Hernandez A, Varghese N, McClain KL, Karam LB, Nahmod K, Makedonas G, Mace EM, Sorte HS, Perminow G, Rao VK, O'Connell MP, Price S, Su HC, Butrick M, McElwee J, ... Cooper MA. Early-onset lymphoproliferation and autoimmunity caused by germline STAT3 gain-of-function mutations. *Blood* 2015 **125** 591–599. (doi:10.1182/blood-2014-09-602763)
6. Flanagan SE, Haapaniemi E, Russell MA, Caswell R, Lango Allen H, Franco E De, McDonald TJ, Rajala H, Ramelius A, Barton J, Heiskanen K, Heiskanen-Kosma T, Kajosaari M, Murphy NP, Milenkovic T, Seppanen M, Lernmark A, Mustjoki S, Otonkoski T, Kere J, Morgan NG, Ellard S, & Hattersley AT. Activating germline mutations in STAT3 cause early-onset multi-organ autoimmune disease. *Nature genetics* 2014 **46** 812–814. (doi:10.1038/ng.3040)
7. Haapaniemi EM, Kaustio M, Rajala HLM, Adrichem AJ van, Kainulainen L, Glumoff V, Doffinger R, Kuusanmaki H, Heiskanen-Kosma T, Trotta L, Chiang S, Kulmala P, Eldfors S, Katainen R, Siitonen S, Karjalainen-Lindsberg ML, Kovanen PE, Otonkoski T, Porkka K, Heiskanen K, Hanninen A, Bryceson YT, Uusitalo-Seppala R, Saarela J, Seppanen M, Mustjoki S, & Kere J. Autoimmunity, hypogammaglobulinemia, lymphoproliferation, and mycobacterial disease in patients with activating mutations in STAT3. *Blood* 2015 **125** 639–648. (doi:10.1182/blood-2014-04-570101)
8. Mogensen TH. STAT3 and the Hyper-IgE syndrome: Clinical presentation, genetic origin, pathogenesis, novel findings and remaining uncertainties. *Jak-Stat* 2013 **2** e23435. (doi:10.4161/jkst.23435)
9. Akira S. Roles of STAT3 defined by tissue-specific gene targeting. *Oncogene* 2000 **19** 2607–2611. (doi:10.1038/sj.onc.1203478)
10. Groner B. Determinants of the extent and duration of STAT3 signaling. *Jak-Stat* 2012 **1** 211–215. (doi:10.4161/jkst.21469)
11. Lorenzini T, Dotta L, Giacomelli M, Vairo D, & Badolato R. STAT mutations as program switchers: turning primary immunodeficiencies into autoimmune diseases. *Journal of leukocyte biology* 2017 **101** 29–38. (doi:10.1189/jlb.5RI0516-237RR)
12. Sal G Del, Manfioletti G, & Schneider C. The CTAB-DNA precipitation method: a

common mini-scale preparation of template DNA from phagemids, phages or plasmids suitable for sequencing. *BioTechniques* 1989 **7** 514–520.

13. Adzhubei I a, Schmidt S, Peshkin L, Ramensky VE, Gerasimova A, Bork P, Kondrashov AS, & Sunyaev SR. A method and server for predicting damaging missense mutations. *Nature methods* 2010 **7** 248–249. (doi:10.1038/nmeth0410-248)
14. Kumar P, Henikoff S, & Ng PC. Predicting the effects of coding non-synonymous variants on protein function using the SIFT algorithm. *Nature protocols* 2009 **4** 1073–1081. (doi:10.1038/nprot.2009.86)
15. Schwarz JM, Cooper DN, Schuelke M, & Seelow D. MutationTaster2: mutation prediction for the deep-sequencing age. *Nature methods* 2014. pp 361–362. . (doi:10.1038/nmeth.2890)
16. Li B, Krishnan VG, Mort ME, Xin F, Kamati KK, Cooper DN, Mooney SD, & Radivojac P. Automated inference of molecular mechanisms of disease from amino acid substitutions. *Bioinformatics (Oxford, England)* 2009 **25** 2744–2750. (doi:10.1093/bioinformatics/btp528)
17. Hecht M, Bromberg Y, & Rost B. Better prediction of functional effects for sequence variants. *BMC Genomics* 2015 **16** S1. (doi:10.1186/1471-2164-16-S8-S1)
18. Becker S, Groner B, & Muller CW. Three-dimensional structure of the Stat3beta homodimer bound to DNA. *Nature* 1998 **394** 145–151. (doi:10.1038/28101)
19. Fang P, Girgis R, Little BM, Pratt KL, Guevara-Aguirre J, Hwa V, & Rosenfeld RG. Growth hormone (GH) insensitivity and insulin-like growth factor-I deficiency in Inuit subjects and an Ecuadorian cohort: functional studies of two codon 180 GH receptor gene mutations. *The Journal of clinical endocrinology and metabolism* 2008 **93** 1030–1037. (doi:10.1210/jc.2007-2022)
20. Hwa V, Nadeau K, Wit JM, & Rosenfeld RG. STAT5b deficiency: lessons from STAT5b gene mutations. *Best practice & research. Clinical endocrinology & metabolism* 2011 **25** 61–75. (doi:10.1016/j.beem.2010.09.003)
21. Wildin RS, Ramsdell F, Peake J, Faravelli F, Casanova JL, Buist N, Levy-Lahad E, Mazzella M, Goulet O, Perroni L, Bricarelli FD, Byrne G, McEuen M, Proll S, Appleby M, & Brunkow ME. X-linked neonatal diabetes mellitus, enteropathy and endocrinopathy syndrome is the human equivalent of mouse scurfy. *Nature genetics*

- 579 2001 **27** 18–20. (doi:10.1038/83707)
- 580 22. Vliet HJJ van der & Nieuwenhuis EE. IPEX as a Result of Mutations in FOXP3.
 581 *Clinical and Developmental Immunology* 2007 **2007** 89017.
 582 (doi:10.1155/2007/89017)
- 583 23. Richards S, Aziz N, Bale S, Bick D, Das S, Gastier-Foster J, Grody WW, Hegde M,
 584 Lyon E, Spector E, Voelkerding K, Rehm HL, & Committee O behalf of the ALQA.
 585 Standards and Guidelines for the Interpretation of Sequence Variants: A Joint
 586 Consensus Recommendation of the American College of Medical Genetics and
 587 Genomics and the Association for Molecular Pathology. *Genetics in medicine :*
 588 *official journal of the American College of Medical Genetics* 2015 **17** 405–424.
 589 (doi:10.1038/gim.2015.30)
- 590 24. Hsu AP, Uzel G, Brodsky N, Freeman AF, Demidowich A, Davis J, Turner ML,
 591 Anderson VL, Darnell DN, Welch PA, Kuhns DB, Ph D, Frucht DM, Malech HL,
 592 Gallin JJ, Kobayashi SD, Ph D, Whitney AR, Voyich JM, Ph D, Musser JM, Ph D,
 593 Woellner C, Sc M, Schäffer AA, Ph D, Puck JM, & Grimbacher B. Mutations in the
 594 Hyper-IgE Syndrome. 2007 1608–1619. (doi:10.1056/NEJMoa073687)
- 595 25. Minegishi Y, Saito M, Tsuchiya S, Tsuge I, Takada H, Hara T, Kawamura N, Ariga
 596 T, Pasic S, Stojkovic O, Metin A, & Karasuyama H. Dominant-negative mutations in
 597 the DNA-binding domain of STAT3 cause hyper-IgE syndrome. *Nature* 2007 **448**
 598 1058–1062. (doi:10.1038/nature06096)
- 599 26. Sediva H, Dusatkova P, Kanderova V, Obermannova B, Kayserova J, Sramkova L,
 600 Zemkova D, Elblova L, Svaton M, Zachova R, Kolouskova S, Fronkova E, Sumnik
 601 Z, Sediva A, Lebl J, & Pruhova S. Short Stature in a Boy with Multiple Early-Onset
 602 Autoimmune Conditions due to a STAT3 Activating Mutation: Could Intracellular
 603 Growth Hormone Signalling Be Compromised?. *Hormone research in paediatrics*
 604 2017 . (doi:10.1159/000456544)
- 605 27. Velayos T, Martinez R, Alonso M, Garcia-Etxebarria K, Aguayo A, Camarero C,
 606 Urrutia I, Martinez de LaPiscina I, Barrio R, Santin I, & Castano L. An Activating
 607 Mutation in STAT3 Results in Neonatal Diabetes Through Reduced Insulin
 608 Synthesis. *Diabetes* 2017 **66** 1022–1029. (doi:10.2337/db16-0867)
- 609 28. Weinreich MA, Vogel TP, Rao VK, & Milner JD. Up, Down, and All Around:

- Diagnosis and Treatment of Novel STAT3 Variant. *Frontiers in pediatrics* 2017 **5** 49. (doi:10.3389/fped.2017.00049)
29. Husby J, Todd AK, Haider SM, Zinzalla G, Thurston DE, & Neidle S. Molecular dynamics studies of the STAT3 homodimer:DNA complex: relationships between STAT3 mutations and protein-DNA recognition. *Journal of chemical information and modeling* 2012 **52** 1179–1192. (doi:10.1021/ci200625q)
 30. Li L & Shaw PE. Elevated Activity of STAT3C due to Higher DNA Binding Affinity of Phosphotyrosine Dimer Rather than Covalent Dimer Formation. *Journal of Biological Chemistry* 2006 **281** 33172–33181. (doi:10.1074/jbc.M606940200)
 31. Herrington J, Smit LS, Schwartz J, & Carter-Su C. The role of STAT proteins in growth hormone signaling. *Oncogene* 2000 **19** 2585–2597. (doi:10.1038/sj.onc.1203526)
 32. Akira S. Functional roles of STAT family proteins: lessons from knockout mice. *Stem cells (Dayton, Ohio)* 1999 **17** 138–146. (doi:10.1002/stem.170138)
 33. Zheng J, Veerdonk FL van de, Crossland KL, Smeekens SP, Chan CM, Shehri T Al, Abinun M, Gennery AR, Mann J, Lendrem DW, Netea MG, Rowan AD, & Lilic D. Gain-of-function STAT1 mutations impair STAT3 activity in patients with chronic mucocutaneous candidiasis (CMC). *European Journal of Immunology* 2015 **45** 2834–2846. (doi:10.1002/eji.201445344)
 34. Eisenberg D, Weiss RM, & Terwilliger TC. The hydrophobic moment detects periodicity in protein hydrophobicity. *Proceedings of the National Academy of Sciences of the United States of America* 1984 **81** 140–144.
 35. Baker NA, Sept D, Joseph S, Holst MJ, & McCammon JA. Electrostatics of nanosystems: application to microtubules and the ribosome. *Proceedings of the National Academy of Sciences of the United States of America* 2001 **98** 10037–10041. (doi:10.1073/pnas.181342398)
 36. Lejarraga H, Pino M del, Fano V, Caino S, & Cole TJ. [Growth references for weight and height for Argentinian girls and boys from birth to maturity: incorporation of data from the World Health Organisation from birth to 2 years and calculation of new percentiles and LMS values]. *Archivos argentinos de pediatria* 2009 **107** 126–133. (doi:10.1590/S0325-00752009000200006)

641 37. Kuczmarski RJ, Ogden CL, Guo SS, Grummer-Strawn LM, Flegal KM, Mei Z, Wei
642 R, Curtin LR, Roche AF, & Johnson CL. 2000 CDC Growth Charts for the United
643 States: methods and development. *Vital and health statistics. Series 11, Data from*
644 *the national health survey* 2002 1–190.

645

646

Supplementary Material

[Click here to download Supplementary Material: Gutierrez et al_Supp.docx](#)